LA-UR-97- - 4036

Title:

NUMERICAL SIMULATION OF TWO WILDFIRE EVENTS USING A COMBINED MODELING SYSTEM (HIGRAD/BEHAVE)

CONF-980121--

RECEIVED
FEB 02 1998
OSTI

Author(s):

J. REISNER, EES-8
J. BOSSERT, EES-8
J. WINTERKAMP, EES-8

Submitted to:

SECOND SYMPOSIUM ON FIRE AND FOREST METEOROLOGY

JANUARY 11-16, 1998

PHOENIX, AZ

DISTRIBUTION OF THIS DOCUMENT IS UNLIMITED

MASTER

19980327 076

Los Alamos
NATIONAL LABORATORY

DTIC QUALITY INSPECTED 3

1.2 NUMERICAL SIMULATIONS OF TWO WILDFIRE EVENTS USING A COMBINED MODELING SYSTEM (HIGRAD/BEHAVE)

Jon Reisner, Jim Bossert, and Judy Winterkamp

Los Alamos National Laboratory *
Los Alamos, NM 87544

1. INTRODUCTION

The ability to accurately forecast the spread of a wildfire would significantly reduce human suffering and loss of life, the destruction of property, and expenditures for assessment and recovery. To help achieve this goal we have developed a model which accurately simulates the interactions between winds and the heat source associated with a wildfire. We have termed our new model HIGRAD or HIgh resolution model for strong GRADient applications. HIGRAD employs a sophisticated numerical technique to prevent numerical oscillations from occurring in the vicinity of the fire. Of importance for fire modeling, HIGRAD uses a numerical technique which allows for the use of a compressible equation set, but without the time-step restrictions associated with the propagation of sound-waves.

HIGRAD is linked to a BEHAVE-like fire model (Andrews 1986; Andrews and Chase 1989). The fire model uses empirical functions (Rothermel 1972, 1991) to determine the rate of fire spread. By design the BEHAVE model is computationally efficient; however, whether a simple empirical model can accurately forecast fire spread is somewhat debatable. In this paper we intend to demonstrate that the BEHAVE model linked to HIGRAD can simulate a wildfire to sufficient accuracy to be of use in the operational arena. We have chosen to simulate two wildfires, the South Canyon fire and the Calabasas fire. In the next section we will give a brief overview of the two fires. In section three we will explain details of the HIGRAD and BEHAVE models and a description of the model setups used for the two simulations. Next, we will show results and finally we will sketch our future plans for transforming the HIGRAD/BEHAVE modeling system into an operational package.

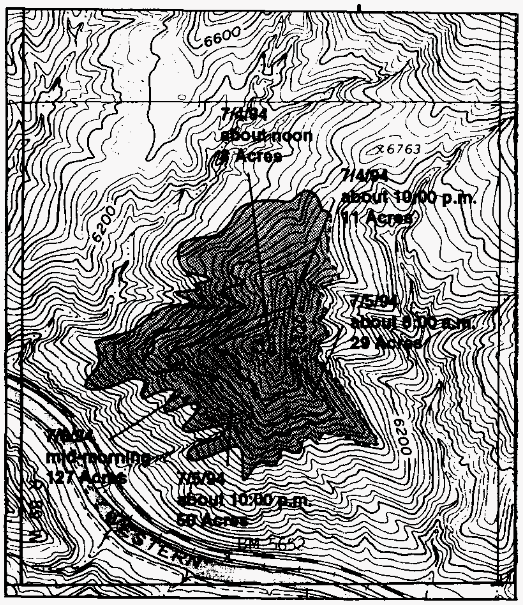

Figure 1. From the U.S. Government Intergency Report on the South Canyon Fire (Rosenkrance et al. 1994). The fire propagation prior to the blowup.

2. OBSERVATIONS

2.1 South Canyon Fire

The South Canyon fire (Rosenkrance et al. 1994) occurred during a 3-day period of July 3-6, 1994. 2000 acres were burned during this fire. The area which burned is located about 7 miles west of Glenwood Springs and just north of Interstate 70. During the last day of the fire, a fire blowup occurred claiming the lifes of 14 firefighters. Prior to this blowup the fire expanded slowly outward from its ignition point—at the base of a ridgeline extending south from Storm King mountain (Fig. 1). On July 6, the fire moved into the bottom of the drainage (point A in Fig. 2) from this point the fire took only 15 minutes to get to the ridge line (Point H in Fig. 2).

Two weather factors were key in allowing for the blowup to occur. First, fire danger indices prior to the blowup were at the highest levels in

---

* Los Alamos National Laboratory is operated by the University of California for the U.S. Department of Energy

---

Corresponding author address: Dr. Jon M. Reisner, Los Alamos National Laboratory, Earth and Environmental Sciences, EES-8, MS D401, Los Alamos, NM 87545

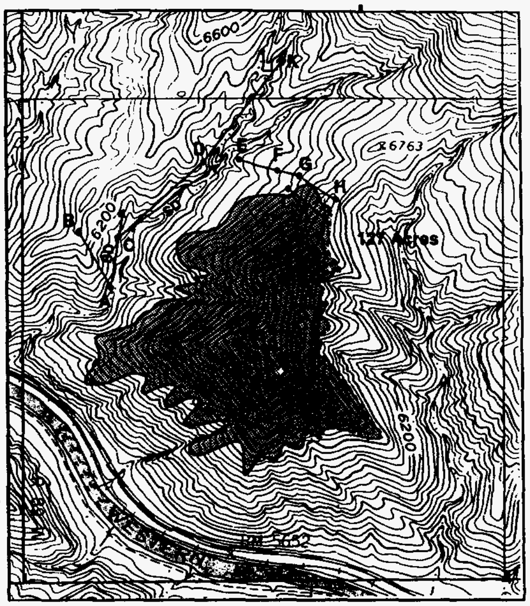

Figure 2. From the U.S. Government Intergency Report on the South Canyon Fire (Rosenkrance et al. 1994). The fire propagation during the blowup.

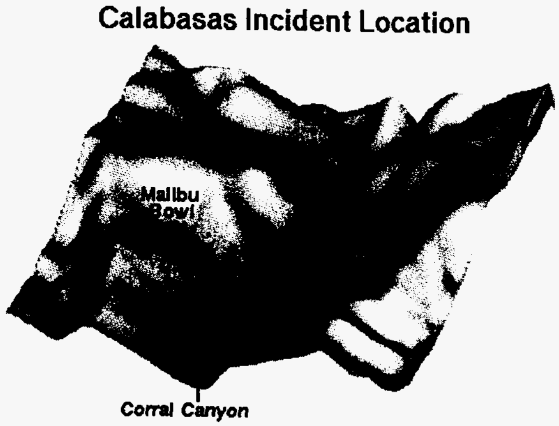

Figure 3. 3-D perspective of Corral Canyon and the location of Malibu Bowl within the canyon.

21 years. Second, a cold front passed over the area on the afternoon of July 6. Strong and gusty winds followed the passage of the cold front. The cold front was associated with the movement of a large upper-level storm system across Colorado (Bossert et al. 1997). The strong winds caused the fire to race up the steep slopes of the drainage. Another factor for the fire blow up was that the Gambel oak understory was tinder dry from being previously burnt (line segment G to H in Fig. 2) and when the new fire encountered this dry fuel the fire spread rate increased dramatically. Outside of this area, the predominant fuel type was pinyon-juniper.

2.2 Calabasas Fire

On October 21, 1996, the Calabasas fire (Bamattre et al. 1997) was started in Calabasas at Los Virgenes Road near the Ventura Freeway by arcing electrical power lines. In two days the fire spread to cover more than 20 square miles. Because of the presence of offshore winds during the first day of the fire, the fire's movement was primarily towards the coast. On the morning of the second day the winds switched to onshore which caused fires burning in several of the canyons to begin moving away from the coast. In particular, a fire burning in Corral Canyon to the south of the Malibu Bowl area (see Fig. 3) was designated as being a region in which a high potential for serious fire behavior existed (Bamattre et al. 1997). This prediction was indeed correct when the fire which was smoldering at the bottom of the Malibu Bowl during the early afternoon suddenly raced up the steep south facing slopes (80% slope) of the Bowl. The intensity and high rate of speed of the fire resulted in one firefighter whom was stationed at the top of the Malibu bowl being seriously burned. Flame lengths during the active portion of this burn were on the order 100 feet. Fuel types on the slopes were primarily Blue Sage and California Sage with life fuel moistures in this brush being extremely low and below the 15 year average for live fuel moistures in the Malibu area.

3. THE HIGRAD/BEHAVE MODEL AND DESIGN OF NUMERICAL SIMULATIONS

3.1 The HIGRAD model

HIGRAD can solve either the compressible or the anelastic form of the Navier-Stokes equations. Because the anelastic option of HIGRAD is not used in the simulations and the option is described elsewhere (Smolarkiewicz and Margolin 1997), we will only describe in detail the compressible option of HIGRAD. The compressible version of HIGRAD solves the flux-form of the Navier-Stokes equations which can be expressed as follows:

$$\frac{\partial G u \rho}{\partial t} + \nabla \cdot (V G \rho u) = -G R_x \qquad (1a)$$

$$\frac{\partial G v \rho}{\partial t} + \nabla \cdot (V G \rho v) = -G R_y \qquad (1b)$$

$$\frac{\partial G w \rho}{\partial t} + \nabla \cdot (V G \rho w) = -G R_z \qquad (1c)$$

$$\frac{\partial G\theta\rho}{\partial t} + \nabla \cdot (VG\rho\theta) = -GR_\theta \qquad (1d)$$

$$\frac{\partial G\rho}{\partial t} + \nabla \cdot (VG\rho) = R_\rho \qquad (1e)$$

$$p = \left[\frac{(\theta\rho R_g)}{p_o^{R_g/C_p}}\right]^{C_v/C_p} \qquad (1f)$$

where u, v, and w are the velocity components in the coordinate system $[x, y, z] = [x_c, y_c, z_c]$ with the subscript c referring to Cartesian coordinates, θ is the potential temperature, ρ is the density, $G = Det\{\, \partial x_c / \partial x\} = (Det\{\, G^{IJ}\}\ )^{-1/2}$ is the Jacobian of transformation with $G^{IJ} = \sum_{K=1}^{3} (\partial x^I / \partial x_c^K)(\partial x^J / \partial x_c^K)$. (1f) is an equation relating the total pressure, p, to variable ρ and θ. The constants, R_g, C_v, and C_p in (1f) are the gas constant for dry air, the specific heat of air at constant volume, and the specific heat of air at constant pressure. The contravariant vertical component of the advective velocity vector $V = u\hat{i} + v\hat{j} + \omega\hat{k}$ which appears as the result of employing a terrain-following coordinate system, $[x, y,$ and $z] = [x_c, y_c, H(z_c - h)/(H - h)]$ with H being the model depth and $h = h(x_c, y_c)$ the model bottom, can be related to the cartesian velocity components by the following relationship, $\omega = G^{13}u + G^{23}v + G^{-1}w$.

The forces R_x, R_y, R_z, R_θ, and R_ρ in (1) are expressed as follows:

$$\begin{aligned} R_x = &-\frac{\partial p'}{\partial x} - G^{13}\frac{\partial p'}{\partial z} + \\ &f\rho(v - v_e) - \hat{f}\rho(w - w_e) - \\ &\alpha\rho(u - u_e) + f_x \end{aligned} \qquad (2a)$$

$$\begin{aligned} R_y = &-\frac{\partial p'}{\partial y} - G^{23}\frac{\partial p'}{\partial z} - \\ &f\rho(u - u_e) - \alpha\rho(v - v_e) + f_y \end{aligned} \qquad (2b)$$

$$\begin{aligned} R_z = &-G^{-1}\frac{\partial p'}{\partial z} - \rho' g + \\ &\hat{f}\rho(u - u_e) - \alpha\rho(w - w_e) + f_z \end{aligned} \qquad (2c)$$

$$R_\theta = -\alpha\rho(\theta - \theta_e) + \rho H \qquad (2d)$$

$$R_\rho = -\alpha(\rho - \rho_e) \qquad (2e)$$

where u_e, v_e, and w_e are the balanced environmental velocity components, $f = 2\Omega sin\varphi$ and $\hat{f} = 2\Omega cos\varphi$ are the z and y components of the Earth rotation vector at the latitude φ, g is the acceleration due to gravity, and $\rho' = \rho - \rho_e$ is the density perturbation with $\rho_e = \rho_e(z_c)$ the environmental density, H is the heat source associated with the wildfire, and the damping forcings appearing in (2) being used to simulate wave-absorbing regions and/or nudging (Davies 1983). In (2a)-(2c) $p' = p - p_e$ is the pressure perturbation with the environmental pressure, $p_e(z_c)$, being calculated using (1f). The frictional terms, f_x, f_y, and f_z, in (2) are parameterized using the first-order subgrid closure of Smagorinsky (1963).

Excluding parameterized forcing terms, the basic algorithm for integrating (1) on a discrete mesh is second-order-accurate in space and time. The chosen mesh is one in which all variables are defined at the same grid position, A-grid. The model uses the method of averaging technique (Reisner and Kao 1997, Nadiga et al. 1996, Madala 1981) to efficiently filter out sound waves from the compressible equation set. Employing this technique the discretized equation set can be expressed as follows:

$$\begin{aligned} u\rho_i^{n+1} = &MPDATA(u\rho_i^n, \bar{\alpha}_{i\pm1/2e_I}^{n+1/2}, G_i) + \\ &DONOR(\bar{R}_x^{n+1/2}, 0.5\bar{\alpha}_{i\pm1/2e_I}^{n+1/2}, G_i) + \\ &-\alpha\rho(u - u_e) + f_x \end{aligned} \qquad (3a)$$

$$\begin{aligned} v\rho_i^{n+1} = &MPDATA(v\rho_i^n, \bar{\alpha}_{i\pm1/2e_I}^{n+1/2}, G_i) + \\ &DONOR(\bar{R}_y^{n+1/2}, 0.5\bar{\alpha}_{i\pm1/2e_I}^{n+1/2}, G_i) + \\ &-\alpha\rho(v - v_e) + f_y \end{aligned} \qquad (3b)$$

$$\begin{aligned} w\rho_i^{n+1} = &MPDATA(w\rho_i^n, \bar{\alpha}_{i\pm1/2e_I}^{n+1/2}, G_i) + \\ &DONOR(\bar{R}_z^{n+1/2}, 0.5\bar{\alpha}_{i\pm1/2e_I}^{n+1/2}, G_i) + \\ &-\alpha\rho(w - w_e) + f_z \end{aligned} \qquad (3c)$$

$$\begin{aligned} \theta\rho_i^{n+1} = &MPDATA(\theta\rho_i^n, \bar{\alpha}_{i\pm1/2e_I}^{n+1/2}, G_i) + \\ &-\alpha\rho(\theta - \theta_e) + \rho H + f_\theta \end{aligned} \qquad (3d)$$

$$\begin{aligned} \rho_i^{n+1} = &MPDATA(\rho_i^n, \bar{\alpha}_{i\pm1/2e_I}^{n+1/2}, G_i) \\ &-\alpha(\rho - \rho_e) \end{aligned} \qquad (3e)$$

where the bar quantities are calculated by the following

$$\bar{\psi}^t = \frac{1}{\Delta t}\int_t^{t+\Delta t} \psi dt \qquad (4)$$

with ψ representing either the advective velocities, $\alpha_{i\pm1/2e_I}$, or the forcing terms, R_i, with both being calculated in a series of first-order predictor steps (Reisner and Kao 1997). Only pressure gradient and Coriolis forces are included in R_i. The temporal averaging technique allows for a timestep of similar magnitude to an anelastic model to be used in the wildfire simulations. A nonoscillatory forward-in-time algorithm, $MPDATA$, (Smolarkiewicz and Grabowski 1990) is used to advect all variables. The monotonicity constraints in

MPDATA have been modified (Schär and Smolarkiewicz 1996) to ensure that scalar variables in the compressible system remain monotone. The *DONOR* cell step in (5) is required to maintain second-order accuracy of the forcing terms (Smolarkiewicz and Margolin 1993). The frictional terms, the absorber terms, and the heating term are not averaged in time with these terms being approximated to the first-order.

3.2 The BEHAVE model

The fire model uses the VOF method (Margolin et al. 1997) to track the movement of a fireline across a computation cell. In principle, VOF is an Eulerian approach, as it does not track explicitly material interfaces. Instead, it reconstructs such interfaces using auxiliary dependent variables—the partial volume fractions of immiscible materials within computational cells. For example, a partial volume fraction of 0.5 would indicate that one half of the cell is burning with the fireline's orientation being determined by taking local gradients of the partial volume fractions (eq. 12 in Margolin et al. 1997). The fireline's location within a cell can be determined analytically given the orientation and the value of the partial volume fraction. Unlike in Margolin et al., the current application of the VOF technique does directly influence the advection of scalar quantities; does not use advective velocities to advect the interface; and does not conserve total volume. The conservation of total volume would not be expected in a fire which is growing in time.

Instead of using advective velocities to move the interface, the current implementation of the VOF method uses spread rate information obtained from BEHAVE to move the interface. The empirical formulae (Rothermel 1972, 1991) use information such as wind speed, terrain slope, fuel moisture content, and fuel type to determine spread rate and intensity of the fire. Instead of directly coding the formulae into our code, we have chosen to use lookup tables to determine spread rate information. The steps involved in moving the interface are as follows:

1) Flag grids cell which contain an interface or are in the vicinity of an interface.
2) Within flagged cells compute quantities needed for the lookup table: Wind speed, spread direction or the normal direction to the interface with respect to the terrain direction (e.g., interface moving up a slope), and the angle of the wind with respect to the terrain direction. Quantities needed for the lookup table such as terrain slope, fuel type, and fuel moisture content need not be calculated every time step.
3) Call the look up table and determine the individual components of spread by multiplying the spread rate by the angle associated with the direction of spread.
4) Use the individual spread rate components in a donor-cell advection scheme to move the fireline.

In the above approach a split form is used to advect the interface. To minimize splitting errors the starting directions for the 1-D sweeps are alternated. Also, the code contains logic to allow for the interface to not move into grid cells which have been previously burned.

The time rate of change of the partial volume fraction multiplied by the fire intensity is used to estimate the burn rate. For each grid cell there usually is more than one burn rate with the summation of the burn rates being equal to the total heat, H, released in the grid cell. Each burn rate is assigned a start time, t_o, and relative to that start time a particular burn rate is damped by $\exp(t - t_o)$. Vertical distribution of H is accomplished by multiplying H by $\exp(-1./(\text{flameheight})z_c)$ with the flame height being calculated by BEHAVE.

3.3 Design of the numerical simulations

Since the the wildfires occurred during the time period of the day in which a convective boundary layer should have been present, weak background stratification for both environmental profiles of potential temperature and density were imposed during the simulations. The environmental profiles of potential temperature and density used in the simulations were the following:

$$\theta_e = \theta_o exp(Sz_c) \tag{4a}$$

$$\begin{aligned}\rho_e = \rho_o exp(-Sz_c)(1. - g/(C_p T_o S) \\ \times (1. - exp(-Sz_c)) **(1 - C_p/R_g)\end{aligned} \tag{4b}$$

where $\theta_o = 296.0\ K$, $\rho_o = 1.0$ kg m^{-3}, $T_o = 296.0\ K$, and $S = 1.e - 06$ m^{-1}. Environmental profiles of u_e and v_e were assigned to be $u_e = 12$ m s^{-1} and $v_e = 3$ m s^{-1} for the South Canyon simulation and $u_e = 0$ m s^{-1} and $v_e = 4$ m s^{-1} for the Calabasas simulation. The environmental velocity profiles were used in a conjugate-residual solver (Smolarkiewicz and Margolin 1994) capable of generating a potential flow solution consistent with the environmental velocity fields and surface topography. The potential flow field can be used either as an initial wind field for HIGRAD or as a wind field to drive the movement of a fireline produced by the BEHAVE model. Note that BEHAVE can be run independently of HIGRAD. In future simulations, the environmental profiles will be input from a larger scale model such as RAMS (Bossert et al. 1997). A non-rigid lid was used at the top boundary and at the bottom boundary free-slip boundary conditions were specified. A surface drag parameterization was used to mimic the effects of a canopy. Horizontal domain sizes covered an area of 1270 x 1270 m^{-2} for the South Canyon simulation and 1905 x 1905 m^{-2} for the Calabasas simulation resolved with 128 x 128 grid points for each simulation. Vertical resolution was 10 m for both simulations with 101 grid points being used in the vertical. The South Canyon simulation was run for 30 minutes with the simulation being designed to represent the time period in which the actual fire raced up the steep slope. The Calabasas simulation was run for 90 minutes and was designed to simulate the wildfire racing up the steep slopes of the Malibu Bowl. The larger domain of the Calabasas simulation required that a longer simulation time be used. The time step for both simulations was 0.1 s.

For the burn model, a Rothermel fuel type 4, presumably representative of vegetation in both South Canyon and Calabasas was used during the simulations. Live/dead fuel moisture contents of 80%/5% were specified in the BEHAVE model. A horizontally homogeneous fuel bed and moisture content was used for the simulations. Future simulations will use vegetation mapping data from AIRDAS, an airborne scanning instrument, to characterize horizontal variations in fuel type and moisture content. Fuel depth was fixed at 10 m. For the South Canyon wildfire, specification of an initial burnt area was required. The burnt area (Fig 1) was parameterized by a trapeziod with the northwest border of the trapeziod being the only active portion of the fireline. The Calabasas wildfire was initialized by igniting 6 cells in the bottom of Corral Canyon.

Both the HIGRAD and the BEHAVE modules were coded to run efficiently on parallel machines. The parallel platform the simulations were run on was the CRAY T3D at the Advanced Computing Laboratory of Los Alamos National Laboratory. Because of cache problems with the CRAY T3D, the simulations ran about 10 times slower than realtime; however, benchmark simulations run on the new ASCI platform in place at Los Alamos National Laboratory suggest that realtime simulations of wildfire events may now be possible.

4. RESULTS

Even with the rather crude empirical functions employed in the BEHAVE module, the simulations produced results which agree well the observed fire behavior. The total length of time required for the simulated fire to race from the bottom of the South Canyon (Fig. 4) to the ridge line was approximately 18 min. This timing agrees well with the published accounts (Rosenkrance et al. 1994) of the actual fire spread. For the Calabasas fire, the simulated fire moved up the steep slope of Malibu Bowl in a matter of several minutes. For this simulation the heat being released by the fire extended several hundred feet (Fig. 5) above the active fireline. Wind speeds exceeding 25 m s−1 (Fig. 6) were channeled up the terrain chimneys found along the steep slopes of Malibu Bowl. The simulation clearly reveals how intense a wildfire can become on a steep slope. Of note, though the upstream wind fields in the South Canyon and the Calabasas simulations were of differing magnitude, the spread of the respective firelines up steep slopes were of similar magnitude in time. The interplay between weak/strong upstream winds and strong/weak winds induced by the simulated fire resulted in wind fields along the steep slopes which were of similar intensity. We plan to run a simulation of the South Canyon simulation with weak winds to determine how fast the fire would move up the drainage under this flow condition.

5. CONCLUSIONS AND FUTURE WORK

The combined HIGRAD/BEHAVE modeling system has been shown to be a useful tool for determining wildfire propagation. We believe this system to be particularly important for illustrating potential dangers associated with fighting wildfires in steep terrain. We are currently planning to use a version of this modeling system for operational use; however, several tasks are required before this goal becomes a reality. Some of tasks are:

1) Topography, initial weather data, and fuels data will need to be gathered quickly for use in the model. AIRDAS data and topography data can be stored prior to a simulation, but weather data from either a large-scale weather model such as RAMS and/or high-resolution weather data in the vicinity of the fire will need to be processed— including time required to run the weather model—prior to a wildfire forecast.
2) Visualization of the data takes considerable time (Ahrens et al. 1997), and new visualization techniques will need to be developed so that realistic looking results can be displayed in real time.
3) The BEHAVE system will need to be tested against a more robust fire module, FIRETEC (Lin and Harlow 1997), currently being developed. This comparison will pinpoint potential weaknesses in the BEHAVE system and determine the feasibility for using a point functional model to determine fire spread.

REFERENCES

J. Ahrens, P. McCormick, J. Bossert, J. Reisner and J. Winterkamp. Case Study: Wildfire Visualization. In Proceedings of Visualization '97. IEEE Computer Society Press, Los Alamitos, CA, 1997.

Andrews, P.L., and C.H. Chase, 1989:BEHAVE:Fire Behavior Prediction and Fuel Modeling System–Burn Subsystem Part 2, NFES 0277, National Intergency Fire Center, 3822 S. Development Ave., Boise, Idaho 83705.

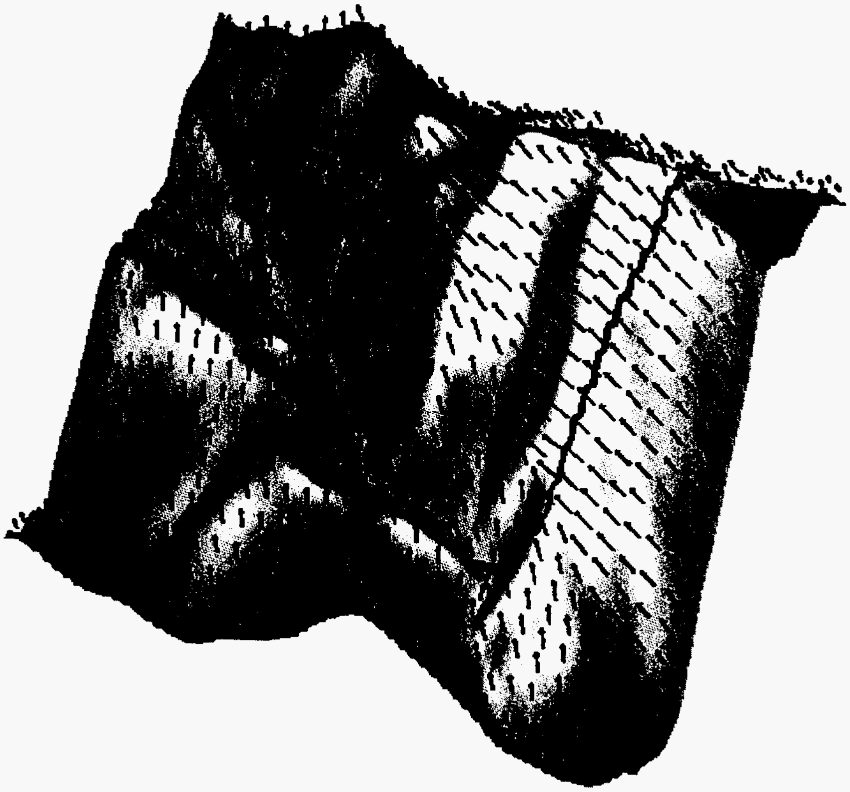

Figure 4. Image of wind vectors, wind speed, and fire perimeter from the South Canyon simulation 10 minutes into the simulation. Lighter shades of grey indicate higher wind speeds.

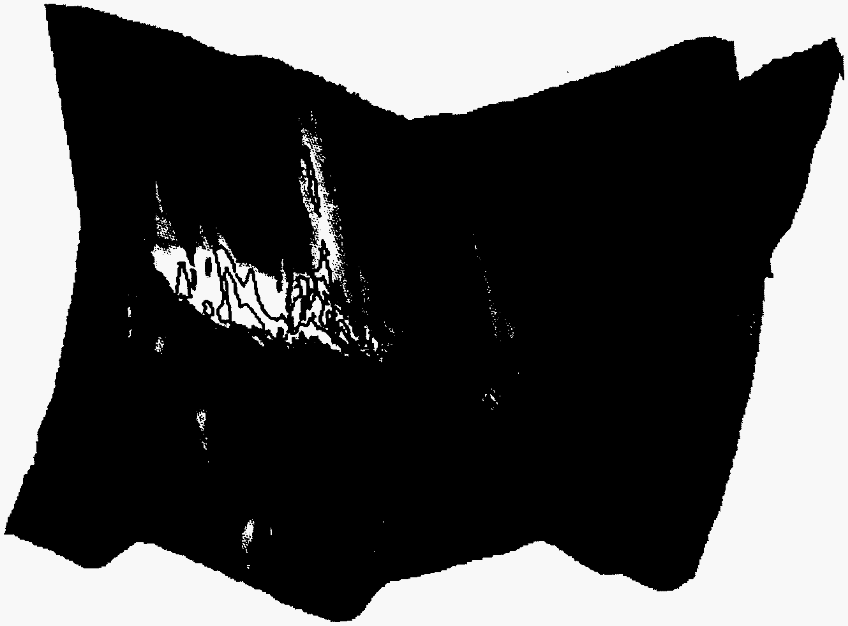

Figure 5. Image of temperature from the Calabasas simulation 30 minutes into the simulation. The east-west vertical cross-section is taken at the top of the Malibu Bowl.

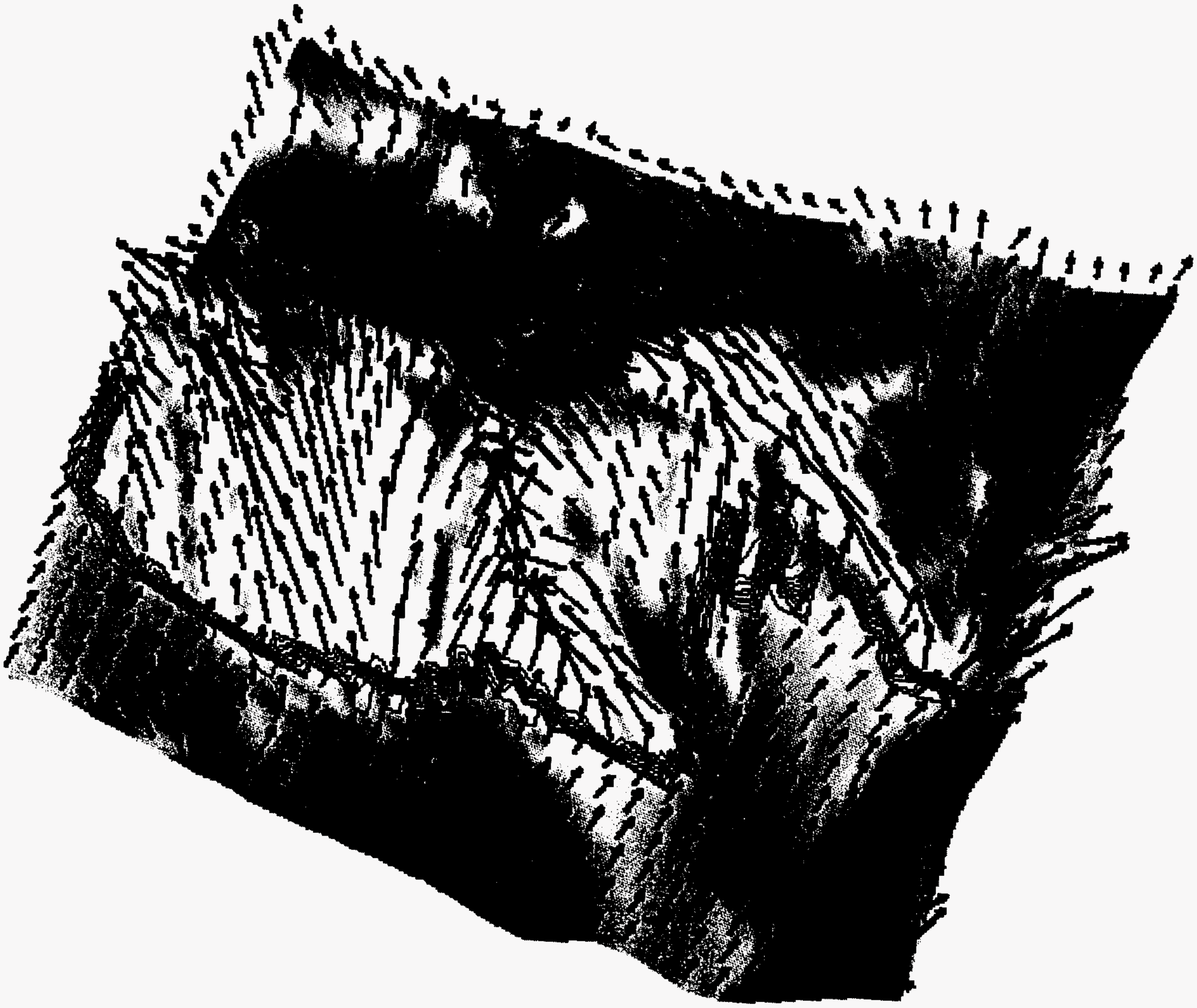

Figure 6. Image of wind vectors, wind speed, and fire perimeter from the Calabasas simulation 30 minutes into the simulation. Lighter shades of grey indicate higher wind speeds.

——, 1986: BEHAVE:Fire Behavior Prediction and Fuel Modeling System–Burn subsystem, Part 1. Gen. Tech. Rep. INT-194. Ogden, UT:U.S. Department of Agriculture, Forest Service, Intermountain Research Station. 130 p.

Bamattre, W., R. Hinz, P.M. Freeman, 1997:Calabasas Incident Entrapment Analysis, Los Angeles County, California.

Bossert, J., F.H. Harlow, R.R. Linn, J.M. Reisner, A.B. White, and J.L. Winterkamp, 1997:Coupled weather and wildfire behavior modeling at Los Alamos: An overview. Second Symposium on Fire and Forest Meteorology. 11-16 January 1998, Phoenix Convention Center, Phoenix Arizona.

Davies, H.C., 1983: Limitations of some common lateral boundary schemes in regional NWP models. *Mon. Wea. Rev.*, **111**, 1002-1012.

Linn, R., and F.H. Harlow, 1997:FIRETEC: A transport model for investigating self-determining wildfire. Second Symposium on Fire and Forest Meteorology. 11-16 January 1998, Phoenix Convention Center, Phoenix Arizona.

Madala, R. V., 1981: Efficient time integration schemes for atmosphere and ocean models. *Finite-difference Techniques for Vectorized Fluid Calculations*, D. Book, Ed., Springer-Verlag, 56-74.

Margolin, L., J. Reisner, and P.K. Smolarkiewicz, 1997: Application of the volume-of-fluid method to the advection-condensation problem. *Mon. Wea. Rev.*, **125**, 2265-2273.

Nadiga B.T., Hecht M.W., Margolin L.G., and P.K. Smolarkiewicz, 1996: 'Preliminary aspects of the method of averaging for the numerical treatment of multiple time sca le systems', LA-UR-96-2409.

Reisner, J., and C.-Y.J. Kao, 1997: Application of simple numerical techniques for increasing the efficiency of a forward-in-time shallow water code on a sphere. *Parallel Computational Fluid Dynamics Algorithms and Results Using Advanced Computers*, Elsevier, New York.

Rosenkrance et al., 1994:Interagency report on the South Canyon fire–accident investigation team. Bureau of Land Management and USDA Forest Service.

Rothermel, R.C., 1991:Predicting the behavior and size of crown fires in the Northern Forests. USDA Forest Service Research Paper INT-438, Intermountain Forest and Range Experiment Station, Ogden, UT.

Rothermel, R.C., 1972:A mathematical model for predicting fire spread in wildfire fuels. USDA Forest Service Research Paper INT-115, Intermountain Forest and Range Experiment Station, Ogden, UT.

Schär, C., and P.K. Smolarkiewicz, 1996:A synchronous and iterative flux-correction formalism for coupled transport equations. *J. Comput. Phys.*, **128**, 101-120.

Smagorinsky, J. 1963:General circulation experiments with the primitive equations. I. The basic experiment. *Mon. Wea. Rev.*, **91**, 99-164.

Smolarkiewicz, P.K., and L.G. Margolin, 1997: On forward-in-time differencing fo r fluids: An Eulerian/semi-Lagrangian nonhydrostatic model for strati fied flows. *Atmos.-Ocean*, in press.

——, and ——, 1994: Variational solver for elliptic problems in atmospheric flows. *Appl. Math. and Comp. Sci.*, **4**, 527-551.

——, and ——, 1993: On forward-in-time differencing for fluids: extension to a curvilinear framework. *Mon. Wea. Rev.*, **121**, 1847-1859.

——, and W.W. Grabowski, 1990: The multidimensional positive definite advective transport algorithm: Nonoscillatory option. *J. Comput. Phys.*, **86**, 355-375.

M98002670

Report Number (14) LA-UR--97-4036
CONF-980121--

Publ. Date (11) 199710
Sponsor Code (18) DOE/MA, XF
UC Category (19) UC-902, DOE/ER

DOE